

See discussions, stats, and author profiles for this publication at: <https://www.researchgate.net/publication/231683884>

# Polyethylenimine Complexes with Retinoic Acid: Structure, Release Profiles, and Nanoparticles

ARTICLE *in* MACROMOLECULES · AUGUST 2000

Impact Factor: 5.8 · DOI: 10.1021/ma000416x

---

CITATIONS

51

---

READS

22

1 AUTHOR:



Andreas F Thünemann

Bundesanstalt für Materialforschung und -pr...

178 PUBLICATIONS 4,962 CITATIONS

SEE PROFILE

# Polyethylenimine Complexes with Retinoic Acid: Structure, Release Profiles, and Nanoparticles

Andreas F. Thünemann\*

*Institute of Theoretical Physics II, Heinrich Heine University Düsseldorf, Universitätsstr. 1, 40225 Düsseldorf, Germany, and Max Planck Institute of Colloids and Interfaces, Am Mühlenberg, 14476 Golm, Germany*

Jochen Beyermann

*Max Planck Institute of Colloids and Interfaces, Am Mühlenberg, 14476 Golm, Germany*

*Received March 7, 2000; Revised Manuscript Received June 27, 2000*

**ABSTRACT:** In this paper we discuss the preparation of complexes formed by polyethylenimine (PEI) and retinoic acid. The molecular weights of the PEIs were 600, 2000, 25 000, and 750 000 g/mol. All complexes form smectic A-like structures whose orders decrease with increasing molecular weight. The complexes in the bulk material obey Porod's law. Macroscopically oriented multilayer films of the complexes were prepared in a single-step procedure by spin coating and were characterized by X-ray reflectivity. The release of retinoic acid from the films was investigated by FTIR and surface tension measurements. It was found that the release from the complexes with the high molecular weight PEIs is faster than that from the complexes with low molecular weight. Steric stabilized nanoparticles of the complexes were prepared with sizes ranging from 170 to 580 nm by using Poloxamer 188 as the dispersing agent in aqueous media. Their characterization was carried out using dynamic light scattering and atomic force microscopy. It was found that the particle sizes decreased with the increasing molecular weight of the PEIs. Further, the particle structure became more compact with the increasing molecular weight of the PEIs. The particles of the complexes with the lowest molecular weight were assumed to be doughnut-shaped (toroids).

## Introduction

Polyethylenimine is a branched, water-soluble polymer, which is widely used in the paper industry.<sup>1</sup> At low pH values, PEI has the highest known charge density of all polyelectrolytes. PEI is also commercially available in a wide range of molecular weights (600 to 2 000 000 g/mol). Currently numerous efforts in industry and in research institutes are being made in order to develop new applications for this polymer,<sup>1</sup> focusing on novel concepts for areas such as food, cosmetic, and pharmaceutical research. For example, PEI has been reported to promote transgene delivery to the nucleus in mammalian cells,<sup>2</sup> and it has been proposed as a potential gamma scintigraphy imaging agent.<sup>3</sup> In comparison to viral vectors, the vectors formed by PEI–DNA complexes retain high attractiveness in gene therapy due to their theoretically excellent safety profile. In addition to the complexation of DNA, PEI has a strong tendency to form complexes with anionic surfactants.<sup>4</sup> Recently, Kabanov et al. proposed the complex of poly(ethylene oxide)-*g*-polyethylenimine and biologically active surfactants as a novel drug delivery system.<sup>5</sup> Such complexes form “micellar microcontainers” with retinoic acid, a molecule which is very optically active, and from the physicochemical point of view it is considered to be a surfactant. Vitamin A and its analogues, in particular retinoic acid, are involved in the proliferation and differentiation of epithelial tissues and have continued to be used in the treatment of dermatological disorders such as acne, psoriasis, and hyperkeratosis.<sup>6,7</sup> A lot of interest has been focused on

how to understand the role of retinoic acid in cell differentiation. This involves investigating the binding properties of retinoids on specific proteins,<sup>8,9</sup> its role in malignant-tumor inhibition,<sup>10,11</sup> and in its regulation of brain functions.<sup>12</sup> Natural retinoids need to be bound to specific retinoic-binding proteins in order to ensure their protection, solubility, and transport by body fluids. Immobilization is a major problem in administering retinoic acid as a pharmacological agent. One way of achieving such immobilization and protection of retinoic acid is by binding it to a protein, as is the case in nature. A successful way of mimicking nature's strategy was demonstrated by Zanotti<sup>5</sup> et al. when he cocrystallized transthyretin and retinoic acid. This, however, is a difficult and costly procedure. We have developed an easier and less expensive method for the required immobilization of retinoic acid by its complexation with synthetic cationic polyelectrolytes.<sup>13,14</sup> Further, it was shown that nanoparticles of complexes of synthetic polyamino acids with retinoic acid contain an internal smectic A-like structure.<sup>15</sup>

The work presented here is on the immobilization of retinoic acid by PEI with different molecular weights. Our main interest is on the formation of mesomorphous structures, the release of retinoic acid from its complexes, and the formation of nanoparticles.

## Experimental Section

**Materials.** The crystalline *all-trans*-retinoic acid (tretinoin, vitamin A acid) powder and ethanol were purchased from Fluka. The PEIs with different molecular weights were supplied by BASF (Ludwigshaven, Germany). The polymers are highly branched with molar ratios of primary to secondary to tertiary amino groups of 42:35:23 ( $M_w$  = 600 g/mol), 38:35:27 ( $M_w$  = 2000 g/mol), 34:40:26 ( $M_w$  = 25 000 g/mol), and

\* Corresponding author. e-mail: andreas.thuenemann@mpikg-golm.mpg.de.

35:38:27 ( $M_w = 750\,000$  g/mol).<sup>1</sup> The Poloxamer 188 was a gift from ICI (Manchester, UK). All chemicals were used without further purification.

**Complex Formation.** Retinoic acid (100 mg) was dissolved in 20 mL of ethanol. Then 2 equiv of PEI, dissolved in 20 mL of ethanol, was added within 10 min while stirring. The stoichiometry was calculated with respect to the amino functions. The solutions were cast on glass plates. The two-dimensional geometry of the films was stabilized by a glass frame, which was mounted on top of the glass sheet in the same way as in the procedure described earlier.<sup>16</sup>

**Nanoparticle Formation.** Dispersions of nanoparticles in water were obtained by using Poloxamer 188, a nonionic triblock copolymer, as a dispersing agent in a 1:1 weight ratio of Poloxamer 188 to the complexes. The ethanol solution of the complex (5 mL, 0.4% w/w) was added to 15 mL of an aqueous solution of Poloxamer 188 in droplets while this was being treated with ultrasound. The temperature was adjusted to a range between 20 and 26 °C. Each dispersion was treated six times for 30 s with ultrasound of 70 W power. After the ultrasound treatment, the remaining ethanol was removed in a vacuum at 30 °C. Finally, the mixture was purified by a 5  $\mu$ m filter supplied by the Nalgene Co. The resulting dispersions were characterized by dynamic light scattering. The average particle sizes obtained were 580 nm (PEI-600 retinoate), 240 nm (PEI-2000 retinoate), 185 nm (PEI-25000), and 160 nm (PEI-750000 retinoate) in diameter and with polydispersities of about 0.25.

**Thin Film Formation.** Solutions of the complexes (0.4% (w/w)) in ethanol were used for the preparation of thin films. Naturally oxidized silicon wafers served as substrates. The complexes were deposited on the wafers using the spin-coat technique at a speed of 3000 rpm.

**Methods.** The anisotropic optical properties of complex films were examined by using a polarization microscope (Orthoplan-pol, Leitz) with an angle of 90° between polarizer and analyzer. Wide-angle X-ray scattering (WAXS) measurements were carried out with a Nonius PDS120 powder diffractometer using transmission geometry. A FR590 generator was used as the source for Cu K $\alpha$  radiation, monochromatization of the primary beam was achieved by means of a curved Ge crystal, and the scattered radiation was measured with a Nonius CPS120 position sensitive detector. The resolution of this detector in  $2\theta$  was 0.018°. Small-angle X-ray scattering (SAXS) measurements were carried out with an X-ray vacuum camera with pinhole collimation (Anton Paar, Austria, model A-8054) equipped with image plates (type BAS III, Fuji). The image plates were read with a MAC Science Dip-Scanner IPR-420 and IP reader DIPR-420. The X-ray reflectivity was performed with a  $\theta/2\theta$  instrument (Sot/Supernan DF4,  $U = 40$  kV,  $I = 30$  mA,  $\lambda = 0.154$  nm). The beam divergence of the incoming beam was 0.1°, and the resolution in  $2\theta$  was 0.05°. A secondary monochromator selected the Cu K $\alpha$  lines, and a scintillation counter served as detector. Dynamic light scattering measurements were carried out with a submicron particle sizer, model 370 (Nicomp). Standard transmission electron microscopy (TEM) was performed on nanoparticles of the complexes coated with Poloxamer 188. Samples were prepared by pouring a droplet of 0.1% (w/w) aqueous dispersion onto a supporting grid. After the evaporation of the water, the samples were examined with a Zeiss EM 912 Omega TEM. The scanning force microscopy was performed with a Nano Scope IIIa microscope (Digital Instruments, Santa Barbara, CA), operating in tapping mode. The instrument was equipped with a  $10 \times 10$   $\mu$ m E-scanner and commercial silicon tips (model TESP, the force constant was 50 N/m, the resonance frequency was 300 kHz, and the tip radius was smaller than 20 nm). The samples were prepared by letting droplets of diluted aqueous solutions (0.01% w/w) dry on freshly cleaved muscovite mica surfaces at room temperature. IR spectroscopy was performed in reflection on a Bio Rad 6000 FT-IR spectrometer. The samples were prepared as films on an ATR crystal. They were cast from 200  $\mu$ L of 0.4% (w/w) solution in ethanol. Then 20 mL of physiological sodium chloride solution with a pH of 5.5 was poured

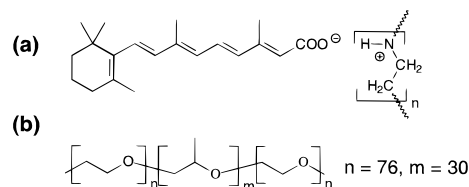


**Figure 1.** Molecular structure of a PEI–retinoate complex (a) and Poloxamer 188 (b), which was used for the formation of nanoparticles.

on top of the films. After this IR spectra were recorded for 8 h at intervals of 2 min. The characteristic absorption band of noncomplexed *all-trans*-retinoic acid at 1255  $\text{cm}^{-1}$  was used as a way of measuring for the release of retinoic acid from the complex.

## Results and Discussion

We used commercially available PEIs with molecular weights of 600, 2000, 25 000, and 750 000 g/mol for complex formation. The resulting complexes are called PEI-600 retinoate, PEI-2000 retinoate, PEI-25000 retinoate, and PEI-750000 retinoate. A sketch of the PEI complexes is shown in Figure 1. Solutions of the PEI–retinoate complexes in ethanol were cast on glass substrates in order to form films. The films of all complexes are soft materials. No glass transition could be found for the PEI–retinoate complexes by differential scanning calorimetry in the temperature range  $-100$  to  $200$  °C. By contrast, complexes of retinoic acid with other polycations, such as poly(ijonene-6,3), poly(*N*-methylene-4-vinylene), and poly(diallyldimethylammonium), have glass-transition temperatures in the range  $-19$  to  $28$  °C.<sup>13,14</sup> The reason for the absence of a glass transition of the PEI–retinoate complexes is not clear. However, noncomplexed polyelectrolytes typically do not display glass transitions; this is due to their highly ionic character. Probably the high charge densities of the PEI chains in their ionic complexes suppress the glass transition.

**Molecular and Supramolecular Structure.** The optical micrographs of the PEI–retinoate complexes observed between crossed polarizers show that all complexes are highly birefringent, with textures that are independent of their molecular weights. An example of a typical texture is shown in Figure 2a. Similar textures are known for some lyotropic lamellar systems of phospholipids.<sup>17</sup> They originate from bilayers that were initially horizontal and corrugate in one or two dimensions to form domes and basins, and each appears as a “Maltese cross”. By contrast, typical textures of elongated crystals are found in the micrograph of noncomplexed *all-trans*-retinoic acid when it is prepared in the same way as the complexes (see Figure 2b). We found that a ratio of amino functions to carboxylic acid groups of about 2:1, or higher, is necessary to prevent the crystallization of parts of the retinoic acid. This finding is in agreement with earlier studies in which it was reported that only the primary and the secondary amino functions could be complexed by surfactants but not the tertiary groups.<sup>18</sup> The amount of the tertiary groups is around 25% in the PEIs used for complexation. This explains why an excess of amino functions, with respect to the carboxylic acid groups, has to be achieved for a complete complexation of the retinoic acid and to avoid crystallinity. Small-angle X-ray scattering measurements, which were carried out on films with thicknesses in the range 0.05–1 mm, were used for a



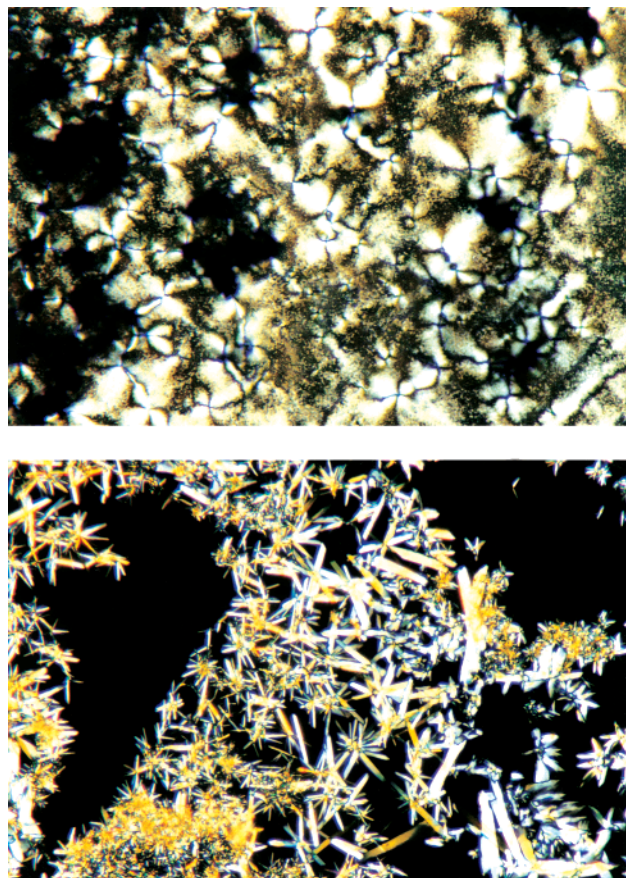


**Figure 2.** Polarization micrograph of a PEI-25000–retinoate complex (upper) and noncomplexed retinoic acid (lower). The samples were prepared from solution in ethanol. The magnification is 50 in both cases.

quantitative comparison of the complexes. An intense Bragg reflection was found in the scattering curves of all complexes at a scattering vector of about  $0.3 \text{ nm}^{-1}$  (not shown). The shapes of the curves were independent of the thicknesses of the films, but they vary with the molecular weight of the PEI. Although no higher order reflections were observed for the complexes in the bulk material, together with the results from polarization microscopy and the fact that in our earlier studies only lamellar structured complexes of retinoic acid were found,<sup>13,15</sup> we propose a lamellar structured mesophase for the PEI–retinoate complexes. This assumption will be confirmed later in the section on thin films. The lamellar spacings increase slightly with the increasing molecular weight of the PEI and were determined to be 3.3 nm (PEI-600), 3.4 nm (PEI-2000), 3.4 nm (PEI-25000), and 3.5 nm (PEI-750000). This indicates higher ordered structures of the complexes with the lower molecular weight PEIs than the complexes with higher molecular weight PEIs. The correlation lengths of the complexes, which were determined from the widths of the reflections, decrease with increasing molecular weight, from about 55 to 41 nm (see Figure 3). This is a further indication for a higher order of the complexes with the PEI of low molecular weight. A probable reason for this influence of the molecular weight PEI on the supramolecular order is that a higher molecular weight would lead to higher packing constraints than a lower molecular weight would do. In addition to the reduction of the order of the lamellar structures, this may lead to different degrees of frustrations.<sup>16</sup> The relations between the order and release profiles of retinoic acid from the

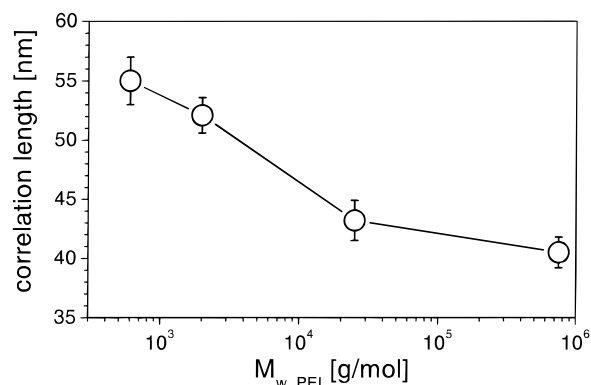


**Figure 3.** Correlation length of the lamellar mesophase of the PEI–retinoate complexes depending on the molecular weight of the PEI.

complex films will be discussed later. In earlier works on polyelectrolyte surfactant complexes it was found that a good model for the description of their mesophase structures could be made by placing the microphase separation into ionic and hydrophobic regions. Often the density transition between these regions is sharp and is similar to that found for strongly segregated block copolymers. Sharp phase boundaries are identified by the presence of Porod's law,<sup>19</sup> which is given by

$$\lim_{s \rightarrow \infty} 2\pi^3 s^4 I(s) = \frac{k}{l_p} \quad (1)$$

The scattering vector is defined as  $s = 2/\lambda \sin \theta$ , and  $\theta$  is the Bragg angle,  $\lambda$  is the wavelength,  $I$  is the scattering intensity,  $l_p$  is the average cord length, and  $k$  is the invariant, which is given by the expression

$$k = 4\pi \int_0^\infty s^2 I(s) ds \quad (2)$$

The scattering intensity is experimentally available between a lower limiting value of the scattering vector  $s_{\min}$  and an upper value  $s_{\max}$ . To calculate the invariant as precisely as possible, the experimental limits were taken into account by approximations of the region of high and low scattering vectors, which results in

$$k = \frac{4}{3}\pi s_{\min}^3 I(s_{\min}) + 4\pi \int_{s_{\min}}^{s_{\max}} s^2 I(s) ds + \frac{4\pi}{s_{\max}} \lim_{s \rightarrow \infty} [s^4 I(s)] \quad (3)$$

A similar approximation for measurements performed with a Kratky camera were earlier used by Ruland.<sup>20</sup> Typically the first and third term in eq 3 sum up together to less than 10% of the invariant. The main source of error in the range of validity covered by Porod's law is the scattering due to density fluctuations and the widths of the domain boundary.<sup>21</sup> The values of  $s^4 I(s)$ , as shown in Figure 4, were found to be constant for a scattering vector in the range  $0.4$ – $0.8 \text{ nm}^{-1}$ . This proves that the structures of the complexes are consistent with Porod's law. A broader transition or a statistical structuring of the domain boundary, as typically observed in microphase-separated block-copolymers,<sup>22</sup> can be excluded. Small deviations from a sharp boundary would indicate a significant deviation from Porod's law.<sup>21</sup> Therefore, we can conclude that the phase boundaries of the complexes are of the order of 1–2

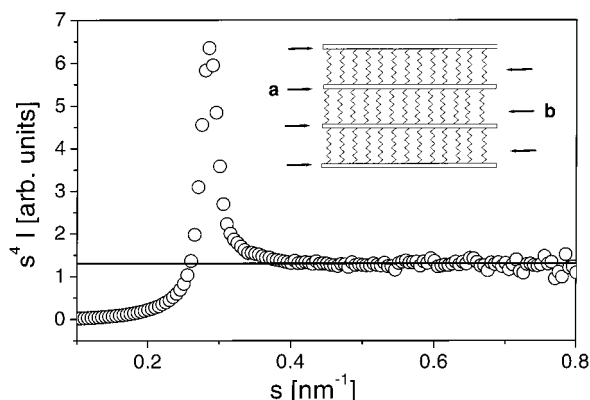


**Figure 4.** Small-angle X-ray scattering intensity in a  $s^4 I(s)$ - $s$  plot (circles). The solid line represents the best fit according to Porod's law at scattering vectors in the range  $0.4$ – $0.8 \text{ nm}^{-1}$ . The scattering vector is defined as  $s = 2/\lambda \sin \theta$ . The inset shows an idealized model of smectic A-like PEI retinoate structures consisting of well-separated supramolecular lamellar sheets: (a) ionic layers with thicknesses of  $0.6 \text{ nm}$  (PEI-600),  $0.7 \text{ nm}$  (PEI-2000 and PEI-25000), and  $0.8 \text{ nm}$  (PEI-750000); (b) nonionic layers with thicknesses of  $2.7 \text{ nm}$  (PEI-600, PEI-2000, PEI-25000, and PEI-750000).

atomic distances. Using eq 1, the average chord lengths were calculated to be  $0.93 \text{ nm}$  (PEI-600),  $1.06 \text{ nm}$  (PEI-2000),  $1.10 \text{ nm}$  (PEI-25000), and  $1.22 \text{ nm}$  (PEI-750000). These values are similar to the polymeric complexes of siloxane surfactants we investigated earlier.<sup>23</sup> The simplest complex structure, which is in agreement with these numbers, is a microphase-separated model constructed from a smaller ionic phase (polyelectrolyte plus ionic headgroups) and a larger nonionic phase (hydrophobic moieties). The slight increase of  $l_p$  with the increasing molecular weight of the PEI is consistent with our assumption that the packing of the structure of the complexes is better for the low molecular weight complexes than for the high molecular weight complexes. We calculated the thicknesses  $d_1$  and  $d_2$  of the lamellae within the smectic A-like structures of the complexes using the relationships<sup>22</sup>

$$d_1 = \frac{L}{2} \left( 1 - \sqrt{1 - \frac{2l_p}{L}} \right), \quad d_2 = L - d_1 \quad (4)$$

which are valid for planar lamellar systems. The values are  $d_1 = 0.6 \text{ nm}$ ,  $d_2 = 2.7 \text{ nm}$  (PEI-600),  $d_1 = 0.7 \text{ nm}$ ,  $d_2 = 2.7 \text{ nm}$  (PEI-2000),  $d_1 = 0.7 \text{ nm}$ ,  $d_2 = 2.7 \text{ nm}$  (PEI-25000), and  $d_1 = 0.8 \text{ nm}$ ,  $d_2 = 2.7 \text{ nm}$  (PEI-750000). We assign  $d_1$  to the ionic lamellae, which are enriched in the polyelectrolytes plus the carboxylic headgroups, and  $d_2$  to the nonionic lamellae, which are enriched in the retinoic acid tails. As expected, the value of  $d_1$  increases slightly with the molecular weight of the PEI, while the value of  $d_2$  does not depend on the weight of the PEI used for complexation. A sketch of the structure is given in Figure 4 (inset).

**Structure of Thin Films.** Thin films of the complexes on silicon wafers were prepared by the spin-coat technique from solutions of the complexes. The film structures were investigated by X-ray reflectivity. Reflectivity curves of thin films are shown in Figure 5. Similarly to complexes of a fluorinated amphiphile,<sup>24</sup> well-defined double-layer stacks developed within a few seconds simply as a result of the deposition of droplets of the solutions of the complex. The molecular weight of the PEI increases in the line from curve a to d. The

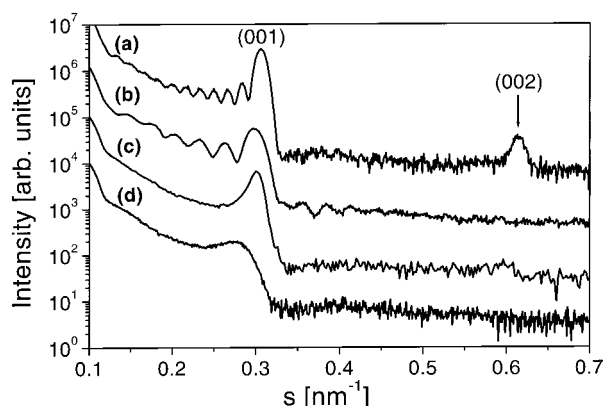


**Figure 5.** X-ray reflectivity curves of thin films of PEI-retinoate complexes at the silicon wafer surfaces. The molecular weights of the PEI used for complexation are  $600$  (a),  $2000$  (b),  $25\,000$  (c), and  $750\,000$  g/mol (d).

presence of Kiessig fringes in curves a and b indicates smooth films for the complexes PEI-600-retinoate and PEI-2000-retinoate. No Kiessig fringes were observed for the complexes with the PEI of the higher molecular weights (curves c and d). A clear second-order maximum is present in the reflectivity curve of PEI-600-retinoate, which proves the assumptions of a lamellar structure of the complex. The long periods of the structures in the films are  $3.3 \text{ nm}$  (PEI-600),  $3.4 \text{ nm}$  (PEI-2000),  $3.4 \text{ nm}$  (PEI-25000), and  $3.6 \text{ nm}$  (PEI-750000). Within the experimental errors these values are in good agreement with those determined for the structures of the complexes in bulk form. Because the same mesomorphous structure was developed in a slow film forming process (solvent casting) and in a fast film forming process (spin coating), we conclude that the time which is necessary for the formation of the mesophase is shorter than the time necessary for the formation of films. The latter is in the order of  $1 \text{ s}$ . The thicknesses of the films formed by the lower molecular weight PEIs were  $80 \pm 2 \text{ nm}$  (PEI-600) and  $47 \pm 2 \text{ nm}$  (PEI-2000) as calculated from the angular positions of the fringes.<sup>25</sup> The reflectivity curves can be explained as resulting from about 25 (PEI-600) and 15 double layers (PEI-2000), respectively. Here the double layer is defined as a structure building block with an ionic sheet covered by nonionic sheets. The latter are formed by the tails of the retinoic acid. In contrast to the complexes of the lower molecular weight PEI, the film surfaces obtained by the complexes of the higher molecular weight PEIs are not sufficiently smooth to produce Kiessig fringes in their reflectivity curves. The correlation length of the lamellar structure in the direction vertical to the wafer surface was determined, from the width of the Bragg peaks, to be  $66 \pm 5 \text{ nm}$  (PEI-25000) and  $32 \pm 5 \text{ nm}$  (PEI-750000). The structure of the films can be explained as consisting of multilayers aligned parallel to the wafer surface. The observation of the macroscopic orientation of the complexes to multilayers with a variability in their order which were produced in a single-step procedure represents, a significant step in the progress of using self-assembly for the preparation of thin organic films. Mechanical fields, present at the spin coating procedure, are probably the reason for the macroscopic orientation of the lamellar stacks parallel to the underlying substrate surface. Such films, when highly loaded with an effective drug, may be useful as a colloidal pharmaceutical formulation.

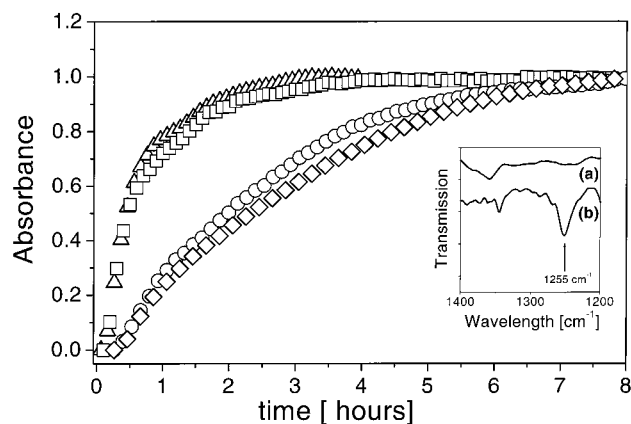


**Figure 6.** Time dependency of the FTIR spectra of the PEI-retinoate complexes at a wavenumber of  $1255\text{ cm}^{-1}$ . The samples are PEI-600-retinoate (diamonds), PEI-2000-retinoate (circles), PEI-25000-retinoate (squares), and PEI-750000 (triangles). The inset shows the transmission of a complex (a) and of noncomplexed retinoic acid (b) around a wavelength of  $1255\text{ cm}^{-1}$ .

**Release Properties.** Films of the complexes are stable in water at a pH of 7 while they dissolve at pH 5. This can be explained by the  $pK_a$  value of retinoic acid, which is, for example, 6.05 in 150 mM NaCl and 6.49 in 5 mM NaCl.<sup>26</sup> Therefore, the anionic retinoic moieties within the complexes will be protonated at pH values lower than the  $pK_a$  which lead to the cleavage of the ionic bonds in the complexes. The first experiments to evaluate the release properties of retinoic acid from thin films of the complexes were performed by using FTIR and surface tension measurements. Films were immersed in solutions of 0.15 *m* sodium chloride at pH 5 for both methods. The increase of the absorbance at  $1255\text{ cm}^{-1}$  (C–O stretch vibration)<sup>27</sup> in the FTIR spectra was used as a qualitative measure for the release of retinoic acid from the PEI-retinoate complexes. For comparison, the spectra of the complex and of the noncomplexed retinoic acid are shown at wavenumbers around  $1255\text{ cm}^{-1}$  (Figure 6, insert curves a and b). The time dependency of the absorbance, which is a relative measure of the amount of released retinoic acid, is shown in Figure 6. It can be seen that the increase of the absorbance, and therefore the release of retinoic acid from the complexes, increases in the line PEI-600, PEI-2000, PEI-25000, PEI-750000. Obviously the release from the complexes with the higher molecular weight PEIs is faster than that from the complexes with the lower molecular weight PEIs. Because the ratio of primary to secondary to tertiary amino functions in all PEIs is approximately the same, we suggest that the different release profiles probably originate from the different supramolecular ordering of the complexes and are not due to the minor differences in their molecular composition. Together with the results from the X-ray reflectivity measurements, it can be concluded that the release of retinoic acid from a complex film is relatively slow for the higher ordered films and relatively fast for the less ordered films. This explains why the release from the complexes with higher molecular weight PEIs is faster than it is from the complexes with the lower molecular weight PEIs.

The molecular structure of retinoic acid is typical for an amphiphilic compound that is concentrated at interfaces. Further, the carboxylic acid groups allow such compounds to adjust their amphiphilic character by the

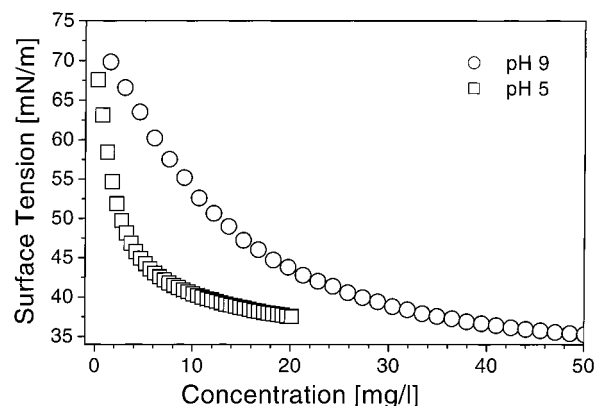


**Figure 7.** Surface tension of *all-trans*-retinoic acid in its protonated state at a pH of 5 (squares) and in its deprotonated state at a pH of 9 (circles).

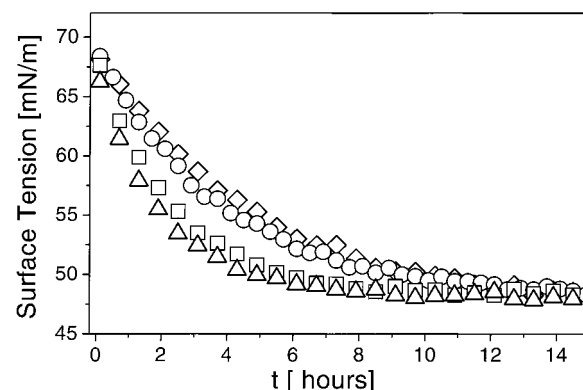


**Figure 8.** Effect of the molecular weight of PEI retinoate complexes on the surface tension of 0.15 *m*/L sodium chloride solutions as a function of time. The samples are PEI-600 retinoate (diamonds), PEI-2000 retinoate (circles), PEI-25000 retinoate (squares), and PEI-750000 (triangles).

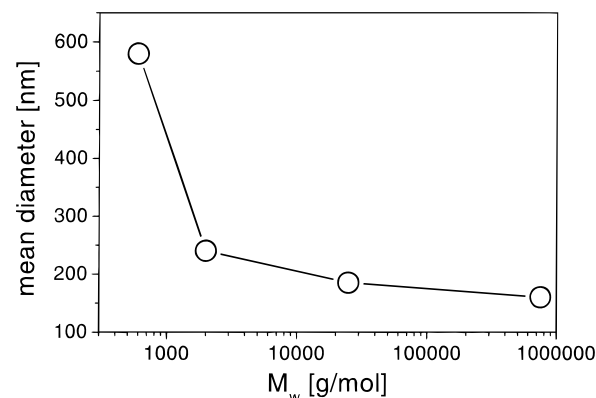


**Figure 9.** Molecular weight dependency of the mean diameter of particles of the PEI-retinoate complexes. The molecular weight is the weight-average of the PEI used for complexation.

degree of their dissociation. Surface tension measurements were carried out in order to determine the surface activity of retinoic acid. Figure 7 shows the surface tension concentration dependence of retinoic acid at  $25\text{ }^{\circ}\text{C}$  in its protonated (pH 5) and deprotonated states (pH 9). As expected, both curves reveal a typical amphiphile. The surface tension with respect to the concentration at pH 5 decreases more strongly than at pH 9. This reflects the fact that the protonated form of retinoic acid is more efficient in its surface activity than the deprotonated form. The critical micell concentrations are  $3.7 \pm 0.5\text{ mg/L}$  (pH 5) and  $19 \pm 2\text{ mg/L}$  (pH 9). The limiting



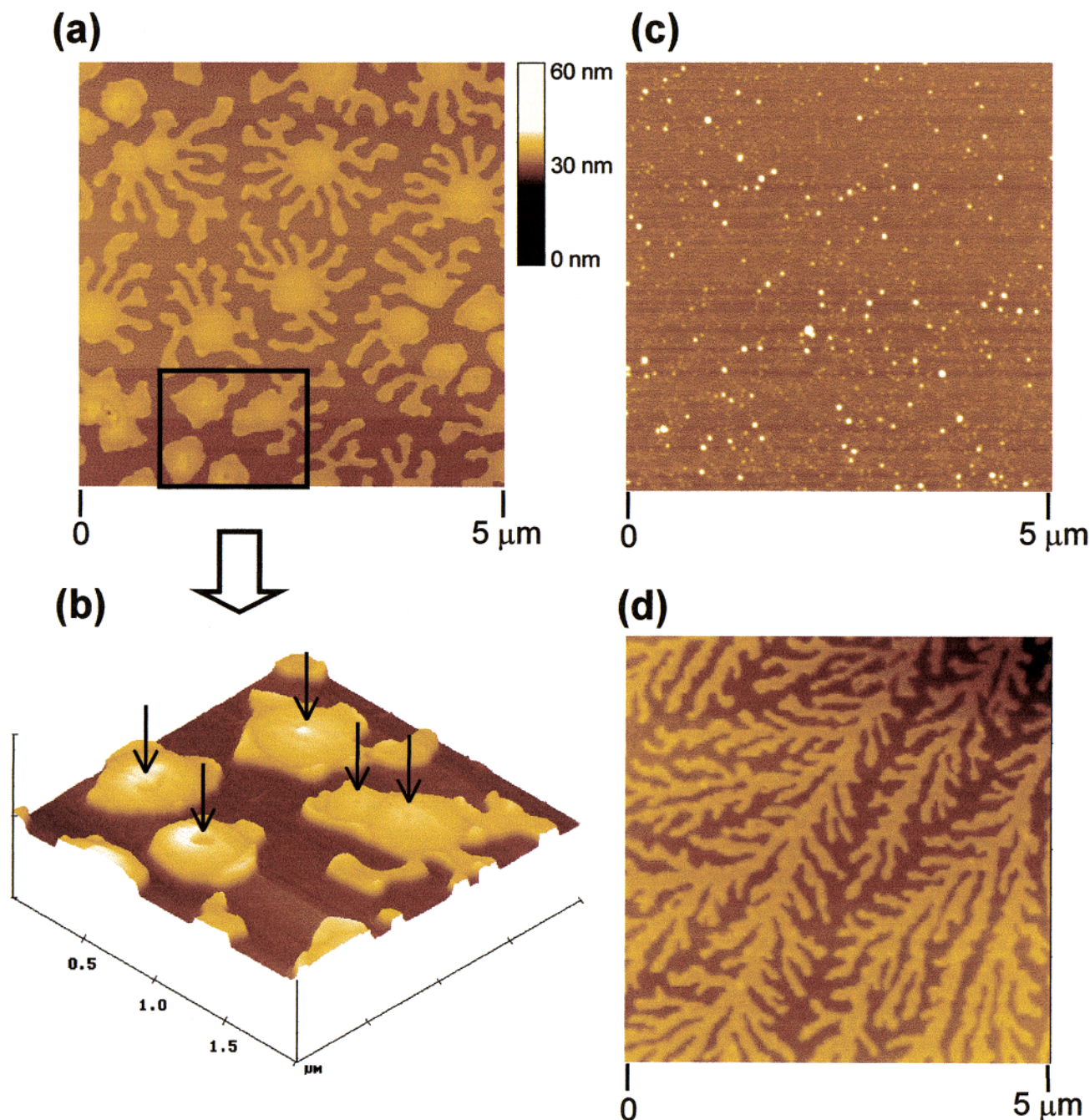


**Figure 10.** AFM images of PEI-retinoate particles dried on mica surfaces. (a) and (c) are top-view images of the PEI-600-retinoate and the PEI-750000-retinoate, respectively. The bird's-eye view (b) is a magnification of (a) enclosed in the plotted rectangle. Arrows in (b) indicate the depressions in the center of the particles. (d) is the top view of Poloxamer 188 after the aqueous solution had been dried out.

surface tension values in both curves is about 35 mN/m. Because of the precipitation of retinoic acid, the highest concentration in the surface tension curve at a pH of 5 was 20 mg/L. By contrast, the solubility at pH 9 is at least 1 g/L. To verify the results from the FTIR measurements, films of the complexes were immersed in a solution of 0.15 mol/L sodium chloride at pH 5. It can be seen in Figure 8 that the surface tension decreases with time when the films were inserted in the solutions. The decrease is steeper the higher the molecular weight of the PEI is. The final value of the surface tension for all films is around 48 mN/m. This corresponds to a maximum concentration of about 2 mg/L, which is below the critical micelle concentration for retinoic acid. We interpret the reduction of the surface

tension to be due to the release of retinoic acid from the films. The release is faster for the higher molecular weight PEI complexes than for the lower. Because the limiting values of the surface tensions are independent of the molecular weight of the PEIs, we conclude that the kinetics of the release are affected by the PEI used, but not the overall amount of released retinoic acid. This is consistent with the results from the FTIR spectroscopy and with our assumption that the complexes differ only in their supramolecular orders.

**Nanoparticles.** The formation of the nanoparticles of the complexes was carried out with the aid of Poloxamer 188, a triblock copolymer, consisting of two poly(ethylene oxide) blocks and a poly(propylene oxide) block (see Figure 1). Poloxamer 188 is a common

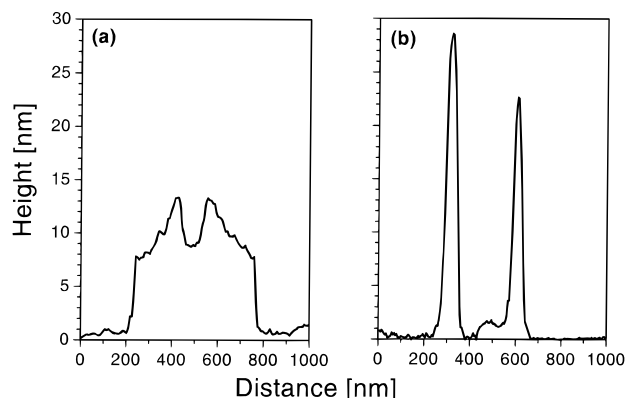


**Figure 11.** Height profiles of the cross section of nanoparticles formed by PEI-600–retinoate (a) and PEI-750000–retinoate (b).

nonionic surfactant frequently used as a steric stabilizer in pharmaceuticals and has proved to be capable of stabilizing nanoparticles.<sup>28–30</sup> The diameters of the particles, as determined by dynamic light scattering, are shown in Figure 9. Surprisingly, the diameters decrease with the increasing molecular weight of the PEI in the line PEI-600 (580 nm), PEI-2000 (240 nm), PEI-25000 (185 nm), PEI-750000 (160 nm). The polydispersities are about 0.25. The sizes were checked by electron microscopy (not shown). Park and Choi<sup>31</sup> have shown that the structures of the PEIs are randomly branched, but they become more compact with increasing molecular weight. Probably the unexpected size dependency of the nanoparticles reflects the structural properties of branched PEI. On the basis of this hypothesis, it must be expected that PEI-750000 retinoate forms a significantly more compact particle structure than PEI-600 retinoate. AFM measurements, carried out on dried PEI retinoate particles, confirmed the expectation of an increase in compactness of the particles with increasing molecular weight. Examples are shown in Figures 10 and 11. It was found that the higher the molecular weight of the PEI, the more compact are the particles. The height profiles of PEI-750000 retinoate (Figures 10c and 11b), for example, are those of typical rigid spheres. The diameters of the particles determined by AFM are about 50 nm smaller than those determined by dynamic light scattering. The higher radii in solution can be explained as an effect of the Poloxamer corona that surrounds the particles, which are swollen in aqueous solution, leading to higher radii in solution than in the dry state. The AFM pictures of the PEI-600 retinoate nanoparticles are unique in their appearance. Here, the particles are collapsed and surrounded by crystalline Poloxamer 188. For comparison, the pure Poloxamer, which was prepared from aqueous solution on mica in the same way as the particles, was investigated. It can be seen in Figure 10b that Poloxamer 188 forms structures which are very similar to those found in the corona of the particles in Figure 10a. A characteristic detail of the PEI-600 retinoate particles is that there are holes in the centers of many of them. They are indicated in the  $2 \times 2 \mu\text{m}$  large bird's-eye view of Figure 10b, pointed by arrows. A typical cross-section profile is shown in Figure 11a. Obviously, the PEI-600 retinoate particles in solution were not homogeneous spheres. Probably these particles may have a doughnut-shape—or toroid—structure in solution, such as described recently by Förster et al. for polyelectrolyte block copolymer micelles.<sup>32</sup> A different morphology of the PEI-600 retinoate

particles can explain why the mean diameter of the particles is significantly higher than that of the other complexes.

## Conclusion

We have shown that the complexes formed by PEI and the amphiphilic drug retinoic acid are lamellar structured materials, which can be processed as lamellar layered ultrathin films as well as nanoparticles. The film-forming properties of the complexes are the better the lower the molecular weight of the PEI is. All complexes are stable in physiological saline at pH 7, whereas retinoic acid is released at pH 5. The higher the molecular weight, the faster its release. With the help of a water-soluble block-copolymer nanoparticles were formed, the size of which decreases with the increasing molecular weight of the PEI. This was explained as a phenomenon induced by the pristine PEI structure. The shapes of the particles from the complexes of the high molecular weight PEI are compact spheres, whereas those of the lowest molecular weights are probably of doughnut-shape or toroid structure.

**Acknowledgment.** The authors thank S. Kubowicz for the X-ray reflectivity measurements and Anne Heilig for AFM measurements. Financial support of the German Science Foundation (Grants Th633/2-1, Lo418/7-1) and the Max-Planck Society is gratefully acknowledged.

## References and Notes

- (1) Information supplied by the manufacturer, BASF, specialty chemicals, Ludwigshafen, Germany.
- (2) Pollard, H.; Remy, J.-S.; Loussouarn, G.; Demolombe, S.; Behr, J.-P.; Escande, D. *J. Biol. Chem.* **1998**, *273*, 7507–7511.
- (3) Nichol, C. A.; Yang, D.; Humphrey, W.; Ilgan, S.; Tansey, W.; Higuchi, T.; Zareneyrizi, F.; Wallace, S.; Podoloff, D. A. *Drug Delivery* **1999**, *6*, 187–194.
- (4) Bronich, T. K.; Cherry, T.; Vinogradov, S. V.; Eisenberg, A.; Kabanov, V. A.; Kabanov, A. V. *Langmuir* **1998**, *14*, 6101–6101.
- (5) Bronich, T. K.; Nehls, A.; Eisenberg, A.; Kabanov, V. A.; Kabanov, A. V. *Colloids Surf. B: Biointerfaces* **1999**, *16*, 243–251.
- (6) Packer, L., Ed.; *Methods in Enzymology*; Academic Press: San Diego, CA, 1990; Vol. 190.
- (7) Lewin, A. H.; Bos, M. E.; Zusi, F. C.; Nair, X.; Whiting, G.; Bouquin, P.; Tetrault, G.; Carroll, F. I. *Pharm. Res.* **1994**, *11*, 192–200.
- (8) Bourguet, W.; Ruff, M.; Chambon, P.; Gonemeyer, H.; Moras, D. *Nature* **1995**, *375*, 377–382.
- (9) Lewin, A. H.; Bos, M. E.; Zusi, F. C.; Nair, X.; Whiting, G.; Bouquin, G. *Pharm. Res.* **1994**, *11*, 192–200.
- (10) Zanotti, G.; D'Acunto, M. R.; Malpeli, G.; Folli, C.; Berni, R. *Eur. J. Biochem.* **1995**, *234*, 563–569.
- (11) Jaeger, E. P.; Jurs, P. C.; Stouch, T. R. *Eur. J. Med. Chem.* **1993**, *28*, 275–283.
- (12) Krezel, W.; Ghyselinck, N.; Samad, T. A.; Dupe, V.; Kastner, P.; Borelli, E.; Chambon, P. *Science* **1998**, *279*, 863–867.
- (13) Patent, PCT/EP98/04644.
- (14) Thünemann, A. *Langmuir* **1997**, *13*, 6040–6046.
- (15) Thünemann, A. F.; Beyermann, J.; Ferber, C.; Löwen, H. *Langmuir* **2000**, *16*, 850–857.
- (16) Antonietti, M.; Conrad, J.; Thünemann, A. F. *Macromolecules* **1994**, *27*, 6007–6011.
- (17) Bougligand, Y. In *Handbook of Liquid Crystals*; Wiley-VCH: Weinheim, 1998; Vol. 1, pp 409–410.
- (18) Bronich, T. K.; Cherry, T.; Vinogradov, S. V.; Eisenberg, A.; Kabanov, V. A.; Kabanov, A. V. *Langmuir* **1998**, *14*, 6101–6106.
- (19) Micha, M. A.; Burger, C.; Antonietti, M. *Macromolecules* **1998**, *31*, 5930–5933.



- (20) Stribeck, N.; Ruland, W. *J. Appl. Crystallogr.* **1978**, *11*, 535–539.
- (21) Siemann, U.; Ruland, W. *Colloid Polym. Sci.* **1982**, *260*, 999–1010.
- (22) Wolff, T.; Burger, C.; Ruland, W. *Macromolecules* **1994**, *27*, 3301.
- (23) Thünemann, A. F.; Lochhaas, K. H. *Langmuir* **1998**, *14*, 6220–6225.
- (24) Thünemann, A. F.; Kubowicz, S.; Pietsch, U. *Langmuir*, in press.
- (25) Holy, V.; Pietsch, U.; Baumbach, T. In *Springer Tracts in Modern Physics*; Springer: Berlin, 1999; Vol. 149..
- (26) Han, C.-H.; Wiedmann, T. S. *Int. J. Pharm.* **1998**, *172*, 241–253.
- (27) Rockley, N. L.; Halley, B. A.; Rockley, M. G.; Nelson, E. C. *Anal. Biochem.* **1983**, *22*, 314–321.
- (28) Douglas, S. J.; Davis, S. S. *J. Colloid Interface Sci.* **1985**, *103*, 154.
- (29) Lechmann, T.; Reinhart, W. H. *Clin. Hemorheol. Microcirc.* **1998**, *18*, 31.
- (30) Pons, M.; Garcia, M. L.; Valls, O. *Colloid Polym. Sci.* **1991**, *269*, 855.
- (31) Park, I. H.; Choi, E. J. *Polymer* **1996**, *37*, 313–319.
- (32) Förster, S.; Hermsdorf, N.; Leube, W.; Schnablegger, H.; Regenbrecht, M.; Akari, S.; Lindner, P.; Bottcher, C. *J. Phys. Chem. B* **1999**, *103*, 6657–6668.

MA000416X